Romanian Reports in Physics **73**, 101 (2021)

GEOMETRIC DISCORD FOR A DRIVEN TWO-QUBIT SYSTEM

TATIANA MIHAESCU[1,2], ELENA CECOI[3], MIHAI A. MACOVEI[3], AURELIAN ISAR[1,2]

[1]Horia Hulubei National Institute of Physics and Nuclear Engineering, 30 Reactorului, POB-MG6, Bucharest-Magurele, Romania
[2]Faculty of Physics, University of Bucharest, 405 Atomistilor, POB-MG11, Bucharest-Magurele, Romania
[3]Institute of Applied Physics, Academiei str. 5, MD-2028 Chişinău, Republic of Moldova
email: macovei@phys.asm.md, isar@theory.nipne.ro

Received October 28, 2020

Abstract. We employ a rescaled version of the geometric measure of quantum discord, based on the Hilbert-Schmidt norm, to calculate it in the steady-state for a concrete system formed of a closely packed and laser-pumped pair of identical two-level qubits being initially uncorrelated and located in their ground states, respectively. Furthermore, the qubits are longitudinally coupled with a single-mode boson field, while both subsystems are damped *via* their corresponding environmental reservoirs. Although the employed metric is still noncontractive under quantum operations, it was shown previously in a series of physical examples that this measure of quantum correlations is in agreement with other discord measures.

Key words: geometric quantum discord.

1. INTRODUCTION

Quantum entanglement represents one of the main resources in performing quantum optics and quantum information processing tasks and protocols [1]. At the same time, in physical phenomena involving mixed states, new types of quantum correlations (QC) have been introduced, in the presence and even in the absence of entanglement, like quantum discord [2–6], and they can exist in any state of a composite system which cannot be described by classical probability theory.

Presently there exists a large number of measures for discord-type QC [7–9], which belong to two main groups: entropic measures, like the quantum discord [2, 3], and geometric measures, such as the geometric discord [10]. The entropic measures provide usually a thermodynamical interpretation of QC [11–21], while the geometric measures of QC are introduced by choosing a metric in the Hilbert space of the considered system, and then one employs it to estimate the distance between the state under scrutinity and the set of classical (non-discordant) states [22]. Usually, the geometric discord is associated to the Hilbert-Schmidt metric [10, 23] and it was applied on several protocols [24, 25]. In [10] it was proposed a geometrical way of quantifying quantum discord, and for two qubits this results in a closed form of expression

for discord.

As remarked in Ref. [26], the geometric discord presents two pathologies which diminish its role as a reliable QC measure. The first one is related to the fact that geometric discord can increase when the unmeasured party is allowed to undergo a non-unitary evolution (described by a completely positive local operation) [27], in contradiction to what happens when one uses the entropic measure [18]. This behaviour is related to the non-contractivity property of the Hilbert-Schmidt norm [28]. Consequently, the geometric discord may only be interpreted as a lower bound to a well-behaved measure of QC [26]. The second pathology arises in the case of high-dimensional systems [25, 26]. It was shown that highly mixed states containing non-zero entropic discord can have negligible geometric quantum discord [25, 29–31]. This behaviour is related too to the Hilbert-Schmidt distance, which is highly sensitive to the purity of states. Both these problems may be fixed by choosing other metrics, like trace distance or Bures distance, which are mathematically well behaved, however, in the majority of cases it is not possible to reach an explicit computability [7].

In Ref. [32] the authors proposed an improved geometric measure of QC, based on the use of the same Hilbert-Schmidt norm. Namely, they derived a computable QC geometric quantifier based on Hilbert-Schmidt distance, and described its behaviour in some examples where the original geometric discord was proven to be meaningless. In all these cases it was observed that the improved geometric measure behaves similarly to the entropic discord, therefore it could provide a meaningful quantifier of discord-like QC. However, the newly introduced indicator still manifests a non-contractive behaviour in quantum channels. Nevertheless, in studying the behaviour of discord-like correlations, the improved measure seems to be preferable to the original geometric discord.

In the present paper, we discuss the geometric quantum discord and its properties for a pair of dipole-dipole interacting two-level qubits which are initially uncorrelated and being in their ground states, respectively. Furthermore, the qubit subsystem is continuously laser-pumped at resonance and longitudinally coupled with a leaking boson mode, respectively. The cooperative spontaneous emission of excited quantum emitters is considered as well. We have found non-zero long-time values for the geometric discord, adjusted geometric discord as well as rescaled geometric discord, respectively, when the frequency of the boson mode is close to the dipole-dipole frequency shift. This demonstrates the existence of quantum correlations in the examined system. Notice that the comparison of Hilbert-Schmidt and trace distance discord in a system of independent two-level atoms with time evolution given by the dissipative process of spontaneous emission was investigated in [33]. The quantum-discord-triggered superradiance and subradiance in a system of two separated atoms was demonstrated as well, in [34]. Furthermore, the interconnection among quantum

correlations between each qubit in a two-atom system and the environment in terms of interatomic distance *via* the quantum discord and entanglement was established in [35]. Depending on the specific initial preparation of the qubits, the properties of the geometric discord were examined in [36].

The paper is organised as follows. In Section 2 we review the main properties of the geometric discord, and introduce a computable geometric measure for the geometric discord and its improved forms, namely, the adjusted geometric discord and rescaled geometric discord. In Section 3 we describe the system of interest for which the quantum discord is calculated and analyse the obtained results in Section 4. We finalise the article with the Summary presented in Section 5.

2. GEOMETRIC QUANTUM DISCORD

We denote by ρ the density operator of a bipartite quantum state in a Hilbert space $\mathcal{H}_{AB} = \mathcal{H}_A \otimes \mathcal{H}_B$. For a bipartite state ρ, the geometric discord with measurements on A [10] was originally defined as the distance between the state and the set of classical-quantum states of the form

$$\chi = \sum p_i |i\rangle_A\langle i| \otimes \rho_B^i, \tag{1}$$

where $\sum_i p_i = 1$ and $\{|i\rangle\}$ is an orthonormal vector set. It can also be defined as the minimum (squared) distance between the state and the set of post-measurement states obtained after a local projective measurement:

$$\mathcal{D}_G(\rho) = \alpha_A \min_{\Pi} \|\rho - \Pi[\rho]\|^2, \tag{2}$$

where $\Pi[\rho] = \sum_i \Pi_i \rho \Pi_i$ is the post-measurement state, $\{\Pi_i\}$ is a complete set of rank-1 projectors on A, and the normalization constant α_A is taken as

$$\alpha_A = \frac{d_A}{d_A - 1}, \tag{3}$$

where $d_A = \dim\{\mathcal{H}_A\}$. When the norm (and hence the distance) used is induced by the Hilbert-Schmidt scalar product, *i.e.*, $\|A\| = \sqrt{\mathrm{Tr}\{A^\dagger A\}}$, the two definitions are equivalent [23], while in general the two geometric approaches may lead to different results. Like the entropic discord, the geometric measure vanishes for classical-quantum states and can increase when a completely positive trace preserving (CPTP) map is applied to the measured subsystem. In addition, due to the choice of the Hilbert-Schmidt metric, its evaluation is less difficult compared to the entropic discord; for example, closed analytical expressions have been obtained for general states of $2 \times d$ systems and two-mode Gaussian states [10, 23, 29, 37–40]. However, the choice of the Hilbert-Schmidt metric is responsible for the pathologies mentioned in [26]. Namely, quantum states with different purities have a different Hilbert-Schmidt

norm $\|\rho\| = \sqrt{\mathrm{Tr}\{\rho^2\}}$, which implies that this metric does not provide reliable information about the distinguishability of mixed states. In the context of QC, it follows that it is possible to construct highly discordant (even entangled) states that possess vanishing geometric discord [25]. In addition, as already mentioned, the geometric discord is not monotonically decreasing under CPTP maps on the subsystem B.

In [10] it was proposed the following geometric measure:

$$\mathcal{D}_G(\rho) = \min_{\chi\in\Omega_0}\|\rho-\chi\|^2, \tag{4}$$

where Ω_0 denotes the set of zero-discord states and $\|X-Y\|^2 = \mathrm{Tr}(X-Y)^2$ is the square norm in the Hilbert-Schmidt space. In the following it is shown how to evaluate this quantity for an arbitrary two-qubit state.

Consider the case $\mathcal{H}_\mathrm{A} = \mathcal{H}_\mathrm{B} = \mathbb{C}^2$. We write a state ρ in Bloch representation:

$$\rho = \frac{1}{4}(\mathbb{I}\otimes\mathbb{I} + \sum_{i=1}^{3} x_i\sigma_i\otimes\mathbb{I} + \sum_{i=1}^{3} y_i\mathbb{I}\otimes\sigma_i + \sum_{i,j=1}^{3} T_{ij}\sigma_i\otimes\sigma_j), \tag{5}$$

where $x_i = \mathrm{Tr}\rho(\sigma_i\otimes\mathbb{I})$, $y_i = \mathrm{Tr}\rho(\mathbb{I}\otimes\sigma_i)$ are components of the local Bloch vectors, $T_{ij} = \mathrm{Tr}\rho(\sigma_i\otimes\sigma_j)$ are components of the correlation tensor, and σ_i, $i\in\{1,2,3\}$, are the three Pauli matrices. To each state ρ we associate the triple $\{\vec{x},\vec{y},T\}$. Hence, we have:

$$\mathcal{D}_G(\rho) = \frac{1}{4}(\|\vec{x}\|^2 + \|T\|^2 - k_{\max}), \tag{6}$$

where $\|\vec{x}\|^2 = \sum_{i=1}^{3} x_i^2$, $\|T\|^2 = \mathrm{Tr}T^\mathrm{T}T$ and $k_{\max}$ is the largest eigenvalue of matrix $K = \vec{x}\vec{x}^\mathrm{T} + TT^\mathrm{T}$. $\mathcal{D}_G(\rho)$ is not normalized to one and its maximum value is 1/2 for two-qubit states, so it is natural to consider $2\mathcal{D}_G(\rho)$ as a proper measure [10].

In Ref. [32] it was proposed an alternative metric in the state space for the evaluation of the distance between two density matrices, that was applied to the computation of geometric discord, such that to preserve the low computational demands of the Hilbert-Schmidt metric, and at the same time to avoid its sensitivity to the mixedness of the input states. To treat states of different purities on the same footing, it was proposed to normalize each state by its Hilbert-Schmidt norm. Hence, given two density matrices ρ_1,ρ_2, their distance is defined as

$$d_T(\rho_1,\rho_2) \equiv \left\| \frac{\rho_1}{\|\rho_1\|} - \frac{\rho_2}{\|\rho_2\|} \right\|, \tag{7}$$

where $\|\cdot\|$ indicates the Hilbert-Schmidt norm. The expression (7) is positive, symmetric, satisfies the triangular inequality and $d_T(\rho_1,\rho_2) = 0 \Leftrightarrow \rho_1 = \rho_2$. One may use it to define the rescaled geometric discord $\mathcal{D}_T(\rho)$, by modifying Eq. (2) as follows:

$$\mathcal{D}_T(\rho) = \beta_A \min_{\Pi} d_T(\rho,\Pi[\rho])^2, \tag{8}$$

with β_A a normalization constant dependent on the dimension of $\mathcal{H}_A$. It was shown in Ref. [32] that the projective measurements minimizing the geometric and the

rescaled discord are the same, independently on the dimensionality of the system. This also implies that minimizing Eq. (8) is equivalent to minimizing the distance between the state ρ and the set of classical-quantum states of the form (1), as in the case for the original geometric discord [23]. One can then employ the expression (8), conveniently normalizing it such that the geometric and rescaled discord are equal for pure, maximally entangled states. In this case one obtains

$$\beta_A = \frac{\mathcal{D}_G^{\max}}{2 - 2\sqrt{1 - \mathcal{D}_G^{\max}/\alpha_A}}, \tag{9}$$

where $\mathcal{D}_G^{\max}$ is the value of the geometric discord for a maximally entangled state, equal to 1 if Eq. (3) is chosen. Finally, it follows that [32]

$$\mathcal{D}_T(\rho) = \beta_A \left[2 - 2\sqrt{1 - \frac{\mathcal{D}_G(\rho)}{\alpha_A \mathrm{Tr}\{\rho^2\}}} \right]. \tag{10}$$

This expression shows that the rescaled discord is obtained effectively by renormalizing the original geometric discord by the purity of the input state. For pure states $\mathrm{Tr}\{\rho^2\} = 1$ and therefore the rescaled discord becomes a function of the geometric discord, and reduces in particular to an entanglement monotone.

We observe that it was enough to adjust the geometric discord by just dividing it by the purity of the state, in order to avoid the main pathology mentioned in [26], namely the fact that $\mathcal{D}_G$ can be changed by reversible operations on the unmeasured party. This adjusted geometric discord, defined as

$$\widetilde{\mathcal{D}}_G(\rho) = \frac{\mathcal{D}_G(\rho)}{\mathrm{Tr}\{\rho^2\}}, \tag{11}$$

is a monotonic function of the rescaled discord $\mathcal{D}_T$ Eq. (10).

However, the rescaled geometric measure inherits from $\mathcal{D}_G$ the non-contractivity problem under CPTP evolutions on the unmeasured system. This means that this quantity should be again regarded just as an indicator rather than as an exact measure of QC. Nevertheless, the examples provided in [32] suggest that this lower bound $\mathcal{D}_T$ may be a meaningful estimator of the QC in bipartite states, irrespective of their purity and the dimensionality of the considered systems.

3. A LASER PUMPED PAIR OF TWO-LEVEL QUBITS LONGITUDINALLY COUPLED WITH A LEAKING BOSON MODE

The above mentioned quantities will be calculated for a concrete system, namely, an environmental vacuum mediated dipole-dipole coupled pair of identical two-level $\{|2\rangle_j, |1\rangle_j\}$ quantum emitters $\{j \in q1, q2\}$, resonantly pumped by a coherent laser source. The laser wavelength is sufficiently bigger than the interqubit spatial interval $|\vec{r}_{q_1 q_2}|$,

while the interparticle separation is larger than the linear size of the quantum emitter itself. Because the laser wave-vector is perpendicular to the line connecting the qubits, the later are in an equivalent position with respect to the driving field. Also, we have assumed that the transition frequencies of both qubits are equal and identical to the external pumping source frequency, respectively. Furthermore, the two-level qubits interact with a single boson mode of frequency ω *via* a longitudinal coupling. Correspondingly, the whole system dampens *via* its interaction with the electromagnetic vacuum modes of the surrounding reservoir as well as through the boson mode environmental thermostat, respectively.

The master equation describing this global system in the Born-Markov approximations [41, 42] is given as follows [43]:

$$\frac{d}{dt}\rho(t)+\frac{i}{\hbar}[\bar{H},\rho]=-\sum_{\{j,l\}\in\{q1,q2\}}\gamma_{jl}[S_j^+,S_l^-\rho]-\frac{\kappa}{2}[b^\dagger,b\rho]-\frac{\kappa}{2}\bar{n}[b^\dagger,[b,\rho]]+H.c.. \tag{12}$$

The Hamiltonian characterizing the corresponding coherent quantum dynamics is $\bar{H}=H+H_i$, where

$$H=\hbar\omega b^\dagger b+\hbar\sum_{j\in\{q1,q2\}}g_jS_z^{(j)}(b+b^\dagger), \tag{13}$$

and

$$H_i=\hbar\Omega_{dd}\sum_{j\neq l\in\{q1,q2\}}S_j^+S_l^-+\hbar\sum_{j\in\{q1,q2\}}\Omega_j(S_j^++S_j^-). \tag{14}$$

Here, the qubit operators $S_j^+=|2\rangle_{jj}\langle 1|$, $S_j^-=[S_j^+]^\dagger$ and $S_z^{(j)}=(|2\rangle_{jj}\langle 2|-|1\rangle_{jj}\langle 1|)/2$ obey the commutation relations: $[S_j^+,S_l^-]=2S_z^{(j)}\delta_{jl}$ whereas $[S_z^{(j)},S_l^\pm]=\pm S_j^\pm\delta_{jl}$. The respective boson mode creation, $b^\dagger$, and annihilation, b, operators satisfy the following commutation relations: $[b,b^\dagger]=1$ and $[b,b]=[b^\dagger,b^\dagger]=0$. Further, g_j is the qubit-boson-mode coupling strength whereas Ω_j, $j\in\{q_1,q_2\}$, denotes the standard Rabi frequency, respectively. We shall assume that these quantities are identical for each qubit, *i.e.*, $g_{q_1}=g_{q_2}\equiv g$ and $\Omega_{q_1}=\Omega_{q_2}\equiv\Omega$. Correspondingly, $\gamma_{q1q1}=\gamma_{q2q2}=\gamma/2$ is the single-qubit spontaneous decay rate, while $\gamma_{q1q2}=\gamma_{q2q1}=\gamma\chi_r/2$ describes the radiative coupling among the two-level qubits. Ω_{dd} corresponds to the dipole-dipole interaction potential, respectively. The radiative coupling χ_r goes to zero (unity) for larger (smaller) interparticle separations $|\vec{r}_{q_1q_2}|$ in comparison to the photon emission wavelength. Respectively, Ω_{dd} tends to zero or to the static dipole-dipole interaction potential. Finally, κ is the damping rate of the boson mode, while $\bar{n}$ gives its mean thermal phonon number corresponding to the frequency ω and environmental temperature T.

In the following, we diagonalize the Hamiltonian (14) describing the dipole-

dipole coupled qubit pair interacting as well with an externally applied coherent laser field, using the two-qubit bare states: $|2_{q1}2_{q2}\rangle$, $|2_{q1}1_{q2}\rangle$, $|1_{q1}2_{q2}\rangle$ and $|1_{q1}1_{q2}\rangle$. Hence, we arrive at the corresponding cooperative two-qubit eigenfunctions:

$$\begin{aligned}
|\Psi_4\rangle &= -\bar{a}\{|2_{q1}2_{q2}\rangle + |1_{q1}1_{q2}\rangle\} + \bar{b}\{|2_{q1}1_{q2}\rangle + |1_{q1}2_{q2}\rangle\},\\
|\Psi_3\rangle &= -\bar{c}\{|2_{q1}2_{q2}\rangle + |1_{q1}1_{q2}\rangle\} + \bar{d}\{|2_{q1}1_{q2}\rangle + |1_{q1}2_{q2}\rangle\},\\
|\Psi_2\rangle &= \frac{1}{\sqrt{2}}\{|2_{q1}1_{q2}\rangle - |1_{q1}2_{q2}\rangle\},\\
|\Psi_1\rangle &= \frac{1}{\sqrt{2}}\{|2_{q1}2_{q2}\rangle - |1_{q1}1_{q2}\rangle\}. \qquad (15)
\end{aligned}$$

Here

$$\bar{a} = \frac{(\Omega_{dd} - \lambda_4)/\sqrt{2}}{\sqrt{(\Omega_{dd} - \lambda_4)^2 + 4\Omega^2}}, \quad \bar{b} = \sqrt{\frac{2\Omega^2}{(\Omega_{dd} - \lambda_4)^2 + 4\Omega^2}},$$
$$\bar{c} = \frac{(\Omega_{dd} - \lambda_3)/\sqrt{2}}{\sqrt{(\Omega_{dd} - \lambda_3)^2 + 4\Omega^2}}, \quad \bar{d} = \sqrt{\frac{2\Omega^2}{(\Omega_{dd} - \lambda_3)^2 + 4\Omega^2}},$$

with

$$\lambda_4 = (\Omega_{dd} - \sqrt{\Omega_{dd}^2 + 16\Omega^2})/2, \quad \lambda_3 = (\Omega_{dd} + \sqrt{\Omega_{dd}^2 + 16\Omega^2})/2,$$

whereas other eigenvalues are $\lambda_2 = -\Omega_{dd}$ and $\lambda_1 = 0$, respectively. Substituting the two-qubit dressed-state transformation (15) in the master equation (12), while keeping the slowly varying terms only by assuming that $\omega > g$ with $\omega \approx \lambda_3$ as well as $\Omega_{dd} \gg \gamma$ and $|\lambda_4| \ll |\lambda_2|$, one arrives at the following main equation governing the quantum dynamics of the examined system [43]:

$$\begin{aligned}
\frac{d}{dt}\rho(t) &+ \frac{i}{\hbar}[\bar{H}_0, \rho] = -\frac{\gamma}{2}(1+\chi_r)\Big(2[\bar{c}\bar{d}R_{44} + \bar{a}\bar{b}R_{33} + \frac{\bar{c}}{2\sqrt{2}}(R_{41} - R_{14}),\\
&\{4(\bar{c}\bar{d}R_{44} + \bar{a}\bar{b}R_{33}) + \sqrt{2}\bar{c}(R_{14} - R_{41})\}\rho] + 2(\bar{a}\bar{d} + \bar{b}\bar{c})^2\{[R_{34}, R_{43}\rho]\\
&+ [R_{43}, R_{34}\rho]\} + \bar{a}^2\{[R_{13}, R_{31}\rho] + [R_{31}, R_{13}\rho]\} - \sqrt{2}\bar{a}(\bar{a}\bar{d} + \bar{b}\bar{c})\\
&\times \{[R_{43}, R_{31}\rho] + [R_{13}, R_{34}\rho] - [R_{34}, R_{13}\rho] - [R_{31}, R_{43}\rho]\}\Big)\\
&- \frac{\gamma}{2}(1-\chi_r)\Big(\bar{b}^2\{[R_{32}, R_{23}\rho] + [R_{23}, R_{32}\rho]\} + \bar{d}^2\{[R_{24}, R_{42}\rho]\\
&+ [R_{42}, R_{24}\rho]\} + \frac{1}{2}\{[R_{12}, R_{21}\rho] + [R_{21}, R_{12}\rho]\}\\
&- \frac{\bar{d}}{\sqrt{2}}\{[R_{42}, R_{21}\rho] + [R_{12}, R_{24}\rho] - [R_{24}, R_{12}\rho] - [R_{21}, R_{42}\rho]\}\Big)\\
&- \frac{\kappa}{2}[b^\dagger, b\rho] - \frac{\kappa}{2}\bar{n}[b^\dagger, [b, \rho]] + H.c. \qquad (16)
\end{aligned}$$

Here

$$\bar{H}_0 = \hbar\lambda_4 R_{44} - \hbar\delta b^\dagger b - \hbar\bar{g}(R_{31}b + b^\dagger R_{13}), \tag{17}$$

where $\delta = \lambda_3 - \omega$, whereas $\bar{g} = \sqrt{2}g\bar{c}$. The resulting two-qubit dressed-state operators which enter in Eq. (16) are defined as follows: $R_{\alpha\beta} = |\Psi_\alpha\rangle\langle\Psi_\beta|$, $\{\alpha,\beta \in 1,\cdots,4\}$, and satisfy the standard commutation relations $[R_{\alpha\beta}, R_{\beta'\alpha'}] = R_{\alpha\alpha'}\delta_{\beta\beta'}$ - $R_{\beta'\beta}\delta_{\alpha'\alpha}$. Note that $|\lambda_4| \ll |\lambda_2|$ means also that we deal with rather weaker applied laser fields, *i.e.*, $\Omega/\Omega_{dd} \ll 1$ or the Rabi frequency Ω is of the order of few γ's or even less.

3.1. THE EQUATIONS OF MOTION

With the help of the Master equation (16), one can obtain the following equations of motion describing the whole laser-pumped qubit-pair plus boson mode sample, where the corresponding pumping and damping effects are properly taken into account:

$$\begin{aligned}
\dot{P}_n^{(0)} &= i\bar{g}(P_n^{(4)} - P_n^{(6)}) - \kappa\bar{n}((n+1)P_n^{(0)} - nP_{n-1}^{(0)}) \\
&- \kappa(1+\bar{n})(nP_n^{(0)} - (n+1)P_{n+1}^{(0)}), \\
\dot{P}_n^{(1)} &= i\bar{g}P_n^{(4)} - \kappa\bar{n}((n+1)P_n^{(1)} - nP_{n-1}^{(1)}) \\
&- \kappa(1+\bar{n})(nP_n^{(1)} - (n+1)P_{n+1}^{(1)}) + \gamma_0^{(1)}P_n^{(0)} \\
&- \gamma_1^{(1)}P_n^{(1)} - \gamma_2^{(1)}P_n^{(2)} - \gamma_3^{(1)}P_n^{(3)} + \gamma_{11}^{(1)}P_n^{(11)}, \\
\dot{P}_n^{(2)} &= -\kappa(1+\bar{n})(nP_n^{(2)} - (n+1)P_{n+1}^{(2)}) \\
&- \kappa\bar{n}((n+1)P_n^{(2)} - nP_{n-1}^{(2)}) + \gamma_0^{(2)}P_n^{(0)} \\
&+ \gamma_1^{(2)}P_n^{(1)} - \gamma_2^{(2)}P_n^{(2)} + \gamma_3^{(2)}P_n^{(3)} - \gamma_{11}^{(2)}P_n^{(11)}, \\
\dot{P}_n^{(3)} &= -i\bar{g}P_n^{(6)} + \gamma_0^{(3)}P_n^{(0)} + \gamma_1^{(3)}P_n^{(1)} - \gamma_2^{(3)}P_n^{(2)} \\
&- \gamma_3^{(3)}P_n^{(3)} - \gamma_{11}^{(3)}P_n^{(11)} - \kappa\bar{n}((n+1)P_n^{(3)} \\
&- nP_{n-1}^{(3)}) - \kappa(1+\bar{n})(nP_n^{(3)} - (n+1)P_{n+1}^{(3)}), \\
\dot{P}_n^{(4)} &= -i\delta P_n^{(5)} + 2i\bar{g}n(P_n^{(1)} - P_{n-1}^{(3)}) - \kappa(1+\bar{n})(2P_n^{(6)} \\
&+ (2n-1)P_n^{(4)} - 2(n+1)P_{n+1}^{(4)})/2 + \kappa\bar{n}(2nP_{n-1}^{(4)} \\
&- (2n+1)P_n^{(4)})/2 - \gamma_4^{(4)}P_n^{(4)} + \gamma_8^{(4)}P_n^{(8)}, \\
\dot{P}_n^{(5)} &= -i\delta P_n^{(4)} - \kappa(1+\bar{n})(2P_n^{(7)} + (2n-1)P_n^{(5)} \\
&- 2(n+1)P_{n+1}^{(5)})/2 - \kappa\bar{n}((2n+1)P_n^{(5)} \\
&- 2nP_{n-1}^{(5)})/2 - \gamma_5^{(5)}P_n^{(5)} + \gamma_9^{(5)}P_n^{(9)},
\end{aligned}$$

$$
\begin{aligned}
\dot{P}_n^{(6)} &= -i\delta P_n^{(7)} + 2i\bar{g}(n+1)(P_{n+1}^{(1)} - P_n^{(3)}) - \kappa(1+\bar{n}) \\
&\times \ ((2n+1)P_n^{(6)} - 2(n+1)P_{n+1}^{(6)})/2 + \kappa\bar{n}(2nP_{n-1}^{(6)} \\
&- \ (2n+3)P_n^{(6)} + 2P_n^{(4)})/2 - \gamma_6^{(6)} P_n^{(6)} + \gamma_{12}^{(6)} P_n^{(12)}, \\
\dot{P}_n^{(7)} &= -i\delta P_n^{(6)} - \kappa(1+\bar{n})((2n+1)P_n^{(7)} - 2(n+1) \\
&\times \ P_{n+1}^{(7)})/2 - \kappa\bar{n}((2n+3)P_n^{(7)} - 2nP_{n-1}^{(7)} \\
&- \ 2P_n^{(5)})/2 - \gamma_7^{(7)} P_n^{(7)} + \gamma_{13}^{(7)} P_n^{(13)}, \\
\dot{P}_n^{(8)} &= i(\lambda_4 - \delta)P_n^{(9)} + i\bar{g}nP_n^{(11)} - \kappa\bar{n}((2n+1)P_n^{(8)} \\
&- \ 2nP_{n-1}^{(8)})/2 - \kappa(1+\bar{n})((2n-1)P_n^{(8)} + 2P_n^{(12)} \\
&- \ 2(n+1)P_{n+1}^{(8)})/2 + \gamma_4^{(8)} P_n^{(4)} - \gamma_8^{(8)} P_n^{(8)}, \\
\dot{P}_n^{(9)} &= i(\lambda_4 - \delta)P_n^{(8)} + i\bar{g}nP_n^{(10)} - \kappa\bar{n}((2n+1)P_n^{(9)} \\
&- \ 2nP_{n-1}^{(9)})/2 - \kappa(1+\bar{n})((2n-1)P_n^{(9)} + 2P_n^{(13)} \\
&- \ 2(n+1)P_{n+1}^{(9)})/2 + \gamma_5^{(9)} P_n^{(5)} - \gamma_9^{(9)} P_n^{(9)}, \\
\dot{P}_n^{(10)} &= i\lambda_4 P_n^{(11)} + i\bar{g}P_n^{(9)} - \kappa\bar{n}((n+1)P_n^{(10)} - nP_{n-1}^{(10)}) \\
&- \ \kappa(1+\bar{n})(nP_n^{(10)} - (n+1)P_{n+1}^{(10)}) - \gamma_{10}^{(10)} P_n^{(10)}, \\
\dot{P}_n^{(11)} &= i\lambda_4 P_n^{(10)} + i\bar{g}P_n^{(8)} - \kappa\bar{n}((n+1)P_n^{(11)} - nP_{n-1}^{(11)}) \\
&- \ \kappa(1+\bar{n})(nP_n^{(11)} - (n+1)P_{n+1}^{(11)}) + \gamma_0^{(11)} P_n^{(0)} \\
&- \ \gamma_1^{(11)} P_n^{(1)} - \gamma_2^{(11)} P_n^{(2)} - \gamma_3^{(11)} P_n^{(3)} - \gamma_{11}^{(11)} P_n^{(11)}, \\
\dot{P}_n^{(12)} &= i(\lambda_4 - \delta)P_n^{(13)} + i\bar{g}(n+1)P_{n+1}^{(11)} + \gamma_6^{(12)} P_n^{(6)} \\
&- \ \kappa(1+\bar{n})((2n+1)P_n^{(12)} - 2(n+1)P_{n+1}^{(12)})/2 \\
&- \ \kappa\bar{n}((2n+3)P_n^{(12)} - 2nP_{n-1}^{(12)} - 2P_n^{(8)})/2 \\
&- \ \gamma_{12}^{(12)} P_n^{(12)}, \\
\dot{P}_n^{(13)} &= i(\lambda_4 - \delta)P_n^{(12)} + i\bar{g}(n+1)P_{n+1}^{(10)} + \gamma_7^{(13)} P_n^{(7)} \\
&- \ \kappa(1+\bar{n})((2n+1)P_n^{(13)} - 2(n+1)P_{n+1}^{(13)})/2 \\
&- \ \kappa\bar{n}((2n+3)P_n^{(13)} - 2nP_{n-1}^{(13)} - 2P_n^{(9)})/2 \\
&- \ \gamma_{13}^{(13)} P_n^{(13)}. \qquad (18)
\end{aligned}
$$

The system of equations (18) can be easily obtained if one first get the equations of motion for the variables $\rho_{\alpha\beta} = \langle\alpha|\rho|\beta\rangle$, $\{\alpha,\beta \in 1,\cdots,4\}$ using the master equation (16), namely, $\rho^{(0)} = \rho_{11} + \rho_{22} + \rho_{33} + \rho_{44}$, $\rho^{(1)} = \rho_{11}$, $\rho^{(2)} = \rho_{22}$, $\rho^{(3)} = \rho_{33}$, $\rho^{(4)} = b^\dagger\rho_{31} - \rho_{13}b$, $\rho^{(5)} = b^\dagger\rho_{31} + \rho_{13}b$, $\rho^{(6)} = \rho_{31}b^\dagger - b\rho_{13}$, $\rho^{(7)} = \rho_{31}b^\dagger + b\rho_{13}$, $\rho^{(8)} = b^\dagger\rho_{34} - \rho_{43}b$, $\rho^{(9)} = b^\dagger\rho_{34} + \rho_{43}b$, $\rho^{(10)} = \rho_{14} - \rho_{41}$, $\rho^{(11)} = \rho_{14} + \rho_{41}$, $\rho^{(12)} = \rho_{34}b^\dagger - b\rho_{43}$, and $\rho^{(13)} = \rho_{34}b^\dagger + b\rho_{43}$ [43]. The projection on the Fock states $|n\rangle$, *i.e.*, $P_n^{(i)} = \langle n|\rho^{(i)}|n\rangle$, $\{i \in 0,\cdots,13\}$,

with $n \in \{0, \infty\}$, will lead us to Eqs. (18). The corresponding decay rates are given in the Appendix A.

In order to calculate the discord one requires the elements of the density matrix $\tilde{\rho}_{q_1 q_2}$ which can be represented in the basis $|2_{q1}2_{q2}\rangle$, $|2_{q1}1_{q2}\rangle$, $|1_{q1}2_{q2}\rangle$ and $|1_{q1}1_{q2}\rangle$. These elements are symmetric under the exchange of the qubits sub-systems. Hence, its elements are given as follows:

$$\tilde{\rho}_{q_1 q_2} = \begin{pmatrix} \tilde{\rho}_{11} & \tilde{\rho}_{12} & \tilde{\rho}_{13} & \tilde{\rho}_{14} \\ \tilde{\rho}_{21} & \tilde{\rho}_{22} & \tilde{\rho}_{23} & \tilde{\rho}_{24} \\ \tilde{\rho}_{31} & \tilde{\rho}_{32} & \tilde{\rho}_{33} & \tilde{\rho}_{34} \\ \tilde{\rho}_{41} & \tilde{\rho}_{42} & \tilde{\rho}_{43} & \tilde{\rho}_{44} \end{pmatrix}, \tag{19}$$

where

$$\begin{aligned}
\tilde{\rho}_{11} &= \frac{1}{4}(1+\rho_{11}-\rho_{22}) - \frac{\Omega_{dd}}{4\sqrt{\Omega_{dd}^2+(4\Omega)^2}}(\rho_{33}-\rho_{44}) \\
&- \frac{\bar{a}}{\sqrt{2}}(\rho_{41}+\rho_{14}), \\
\tilde{\rho}_{12} &= \frac{\Omega}{\sqrt{\Omega_{dd}^2+(4\Omega)^2}}(\rho_{33}-\rho_{44}) - \frac{\bar{c}}{\sqrt{2}}\rho_{41}, \\
\tilde{\rho}_{13} &= \tilde{\rho}_{12}, \\
\tilde{\rho}_{14} &= \frac{1}{4}(1+\frac{\Omega_{dd}}{\sqrt{\Omega_{dd}^2+(4\Omega)^2}})\rho_{44} - \frac{\bar{a}}{\sqrt{2}}(\rho_{41}-\rho_{14}) \\
&+ \frac{1}{4}(1-\frac{\Omega_{dd}}{\sqrt{\Omega_{dd}^2+(4\Omega)^2}})\rho_{33} - \frac{1}{2}\rho_{11}, \\
\tilde{\rho}_{21} &= (\tilde{\rho}_{12})^{\dagger}, \\
\tilde{\rho}_{22} &= \frac{1}{4}(1+\rho_{22}-\rho_{11}) + \frac{\Omega_{dd}}{4\sqrt{\Omega_{dd}^2+(4\Omega)^2}}(\rho_{33}-\rho_{44}), \\
\tilde{\rho}_{23} &= \frac{1}{4}(1-\frac{\Omega_{dd}}{\sqrt{\Omega_{dd}^2+(4\Omega)^2}})\rho_{44} - \frac{1}{2}\rho_{22} \\
&+ \frac{1}{4}(1+\frac{\Omega_{dd}}{\sqrt{\Omega_{dd}^2+(4\Omega)^2}})\rho_{33}, \\
\tilde{\rho}_{24} &= \frac{\Omega}{\sqrt{\Omega_{dd}^2+(4\Omega)^2}}(\rho_{33}-\rho_{44}) + \frac{\bar{c}}{\sqrt{2}}\rho_{14}, \\
\tilde{\rho}_{31} &= (\tilde{\rho}_{13})^{\dagger}, \quad \tilde{\rho}_{32} = \tilde{\rho}_{23}, \quad \tilde{\rho}_{33} = \tilde{\rho}_{22}, \quad \tilde{\rho}_{34} = \tilde{\rho}_{24},
\end{aligned}$$

$$\begin{aligned}
\tilde{\rho}_{41} &= (\tilde{\rho}_{14})^{\dagger}, \quad \tilde{\rho}_{42} = (\tilde{\rho}_{24})^{\dagger}, \quad \tilde{\rho}_{43} = (\tilde{\rho}_{34})^{\dagger}, \\
\tilde{\rho}_{44} &= \frac{1}{4}(1+\rho_{11}-\rho_{22}) - \frac{\Omega_{dd}}{4\sqrt{\Omega_{dd}^2+(4\Omega)^2}}(\rho_{33}-\rho_{44}) \\
&+ \frac{\bar{a}}{\sqrt{2}}(\rho_{41}+\rho_{14}).
\end{aligned} \tag{20}$$

4. ESTIMATION OF THE GEOMETRIC QUANTUM DISCORD FOR THE CONSIDERED MODEL

The quantities introduced in the representation of the density matrix (5) can be expressed through the elements of the density matrix (19,20) as follows:

$$\begin{aligned}
x_1 &= \tilde{\rho}_{13}+\tilde{\rho}_{31}+\tilde{\rho}_{24}+\tilde{\rho}_{42}, \\
x_2 &= i(\tilde{\rho}_{13}-\tilde{\rho}_{31}-\tilde{\rho}_{42}+\tilde{\rho}_{24}), \\
x_3 &= 2(\tilde{\rho}_{11}+\tilde{\rho}_{22})-1, \\
y_1 &= \tilde{\rho}_{12}+\tilde{\rho}_{21}+\tilde{\rho}_{34}+\tilde{\rho}_{43}, \\
y_2 &= i(\tilde{\rho}_{12}-\tilde{\rho}_{21}-\tilde{\rho}_{43}+\tilde{\rho}_{34}), \\
y_3 &= 2(\tilde{\rho}_{11}+\tilde{\rho}_{33})-1, \\
t_{11} &= \tilde{\rho}_{23}+\tilde{\rho}_{32}+\tilde{\rho}_{14}+\tilde{\rho}_{41}, \\
t_{22} &= \tilde{\rho}_{23}+\tilde{\rho}_{32}-\tilde{\rho}_{14}-\tilde{\rho}_{41}, \\
t_{33} &= 1-2\tilde{\rho}_{22}-2\tilde{\rho}_{33}, \\
t_{12} &= i(\tilde{\rho}_{32}-\tilde{\rho}_{23}+\tilde{\rho}_{14}-\tilde{\rho}_{41}), \\
t_{21} &= i(\tilde{\rho}_{14}-\tilde{\rho}_{41}-\tilde{\rho}_{32}+\tilde{\rho}_{23}), \\
t_{13} &= \tilde{\rho}_{13}+\tilde{\rho}_{31}-\tilde{\rho}_{24}-\tilde{\rho}_{42}, \\
t_{31} &= \tilde{\rho}_{12}+\tilde{\rho}_{21}-\tilde{\rho}_{34}-\tilde{\rho}_{43}, \\
t_{23} &= i(\tilde{\rho}_{13}-\tilde{\rho}_{31}+\tilde{\rho}_{42}-\tilde{\rho}_{24}), \\
t_{32} &= i(\tilde{\rho}_{12}-\tilde{\rho}_{21}+\tilde{\rho}_{43}-\tilde{\rho}_{34}).
\end{aligned} \tag{21}$$

Using these expressions one can proceed to the calculation of the geometric quantum discord (6), rescaled geometric discord (10) and adjusted geometric discord (11). The normalising parameters (3) and (9) are taken $\alpha_A = 2$ and $\beta = 1+\frac{1}{\sqrt{2}}$ ($d_A = 2$).

Figure 1 illustrates the steady-state behaviours of these quantities as a function of scaled Rabi frequency. One can notice that all the considered measures representing the geometric quantum discord start from a zero value, corresponding to a zero value of the scaled Rabi frequency, and they have a qualitatively similar non-monotonical behaviour, with a pronounced maximum for some definite value of the scaled Rabi frequency, slightly different for each of the three considered expressions

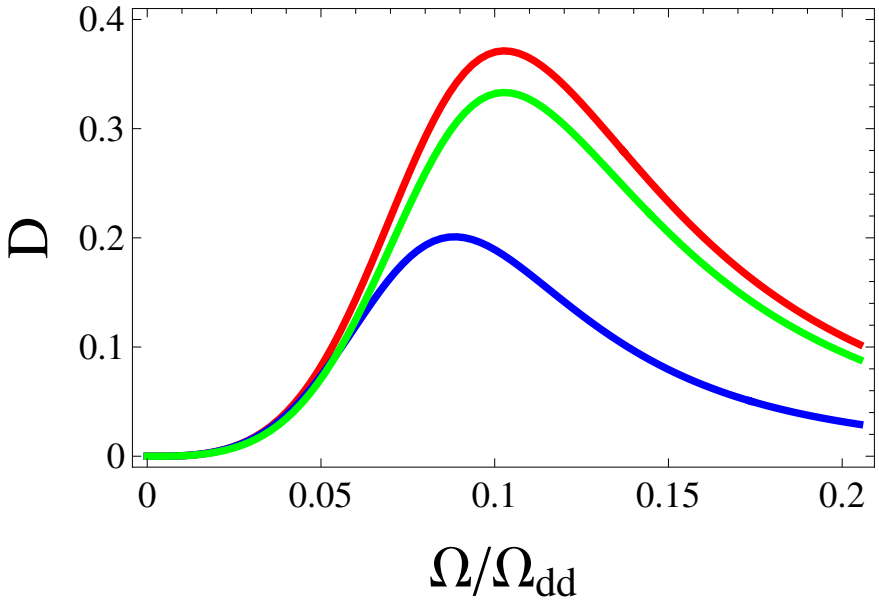

Fig. 1 – (Color online) The steady-state behaviours of all geometric discords discussed in the article, as a function of scaled Rabi frequency Ω/Ω_{dd}. The red curve depicts the adjusted geometric discord based on Eq. (11), while the blue line shows the geometric discord obtained from Eq. (6). The green curve is for the rescaled geometric discord based on Eq. (10), respectively. The involved parameters are: $g/\gamma = 2$, $\Omega_{dd}/\gamma = 28$, $\omega/\gamma = 30$, $\chi_r = 0.98$, $\bar{n} = 20$ and $\kappa/\gamma = 10^{-3}$.

of the geometric quantum discord. One can observe the dependence of the geometric discord on the purity of the global state of the considered system: it has a depressed evolution compared to the adjusted and rescaled discord. In the limit of larger scaled Rabi frequency, all these measures decay asymptotically to a zero value, but geometric discord decays faster than the other two measures – adjusted and rescaled discord.

5. SUMMARY

The study of QC beyond entanglement received in the last years an increasing attention [7]. It is important to distinguish which approaches and methods provide interesting results, and which ones lead to a less correct understanding of the nature and the role of these nonclassical features of quantum states. One one side, employing a QC measure based on the Hilbert-Schmidt distance, like geometric discord, essentially simplifies calculations [10]. On the other side, it manifests a limited reliability and applicative power. When the purity of the global state is not constant, *e.g.*, when the evolution of the system is not unitary, then geometric discord cannot be used as a QC measure [26]. However, using the approach proposed in Ref. [32], it is

possible to correct this behaviour, by identifying the dependence on state purity as the main pathology of the geometric discord, and by proposing a suitable deformation of the Hilbert-Schmidt distance. Other geometric quantifiers, based on contractive distances such as the relative entropy, the trace norm, or the Bures distance, which could generate reliable measures of QC, and could appropriately describe their dynamical evolution [7], however, encounter computational difficulties. The results of Ref. [32] suggest that employing the geometric discord $\mathcal{D}_G$ without a rescaling by the state purity is likely to not lead, in general, to reliable results even in the simplest case of two-qubit states. The rescaled and adjusted discord $\mathcal{D}_T$ were used in the present paper, returning results hopefully in good qualitative and quantitative agreement with those based on other known QC measures, like concurrence. Particularly, we investigated the quantum discord and its properties for a pair of dipole-dipole interacting two-level qubits. The qubit subsystem is initially in its ground state and uncorrelated. Moreover, the qubit subsystem is continuously laser pumped at resonance and longitudinally coupled with a leaking boson mode, respectively. The corresponding damping effects are considered as well. We have found non-zero values in the steady-state for the geometric discord, adjusted geometric discord as well as rescaled geometric discord, respectively, when the frequency of the boson mode is close to the dipole-dipole frequency shift, demonstrating quantum correlations among the two qubits.

Acknowledgements. E.C. and M.A.M. are grateful for the nice hospitality of the Theory Department of the Horia Hulubei National Institute of Physics and Nuclear Engineering, Bucharest, Romania. Furthermore, they acknowledge the financial support from the Moldavian National Agency for Research and Development, grant No. 20.80009.5007.07.

A. THE DECAY RATES ENTERING IN THE EQUATIONS OF MOTION (18)

Below one can find the corresponding decay rates which enter in the Eqs. (18), that is,

$$\begin{aligned}
\gamma_0^{(1)} &= \gamma\bar{c}^2(1+\chi_r),\ \ \gamma_1^{(1)} = \gamma\{(\bar{a}^2+2\bar{c}^2)(1+\chi_r)+(1-\chi_r)/2\},\\
\gamma_2^{(1)} &= \gamma\{\bar{c}^2(1+\chi_r)-(1-\chi_r)/2\},\ \ \gamma_3^{(1)} = \gamma(1+\chi_r)(\bar{c}^2-\bar{a}^2),\\
\gamma_{11}^{(1)} &= \gamma\{(1+\chi_r)(\bar{a}(\bar{a}\bar{d}+\bar{b}\bar{c})/\sqrt{2}+\sqrt{2}\bar{d}\bar{c}^2)+\frac{\bar{d}}{2\sqrt{2}}(1-\chi_r)\},
\end{aligned}$$

$$\begin{aligned}
\gamma_0^{(2)} &= \gamma\bar{d}^2(1-\chi_r),\ \ \gamma_1^{(2)} = \gamma(1-\chi_r)(1/2-\bar{d}^2),\\
\gamma_2^{(2)} &= \gamma(1-\chi_r)(1/2+\bar{b}^2+2\bar{d}^2),\ \ \gamma_3^{(2)} = \gamma(1-\chi_r)(\bar{b}^2-\bar{d}^2),\\
\gamma_{11}^{(2)} &= \gamma\bar{d}(1-\chi_r)/\sqrt{2},
\end{aligned}$$

$$\begin{aligned}
\gamma_0^{(3)} &= 2\gamma(\bar{a}\bar{d}+\bar{b}\bar{c})^2(1+\chi_r),\ \ \gamma_1^{(3)} = \gamma\{\bar{a}^2 - 2(\bar{a}\bar{d}+\bar{b}\bar{c})^2\}(1+\chi_r),\\
\gamma_2^{(3)} &= \gamma\{2(\bar{a}\bar{d}+\bar{b}\bar{c})^2(1+\chi_r) - \bar{b}^2(1-\chi_r)\},\\
\gamma_3^{(3)} &= 2\gamma\{(2(\bar{a}\bar{d}+\bar{b}\bar{c})^2 + \bar{a}^2/2)(1+\chi_r) + \bar{b}^2(1-\chi_r)/2\},\\
\gamma_{11}^{(3)} &= \sqrt{2}\bar{a}\gamma(\bar{a}\bar{d}+\bar{b}\bar{c})(1+\chi_r),
\end{aligned}$$

$$\begin{aligned}
\gamma_4^{(4)} &= \gamma\{(4(\bar{a}\bar{b})^2 + (\bar{a}\bar{d}+\bar{b}\bar{c})^2 + \bar{a}^2 + \bar{c}^2/2)(1+\chi_r) + (1/2+\bar{b}^2)(1-\chi_r)/2\},\\
\gamma_8^{(4)} &= \gamma\{(\sqrt{2}\bar{c}(2\bar{a}\bar{b}+\bar{c}\bar{d}) + \bar{a}(\bar{a}\bar{d}+\bar{b}\bar{c})/\sqrt{2})(1+\chi_r) + \frac{\bar{d}}{2\sqrt{2}}(1-\chi_r)\},
\end{aligned}$$

$$\gamma_5^{(5)} = \gamma_4^{(4)},\ \ \gamma_9^{(5)} = \gamma_8^{(4)},$$

$$\gamma_6^{(6)} = \gamma_5^{(5)},\ \ \gamma_{12}^{(6)} = \gamma_9^{(5)},$$

$$\gamma_7^{(7)} = \gamma_6^{(6)},\ \ \gamma_{13}^{(7)} = \gamma_{12}^{(6)},$$

$$\begin{aligned}
\gamma_4^{(8)} &= \gamma\{(\sqrt{2}\bar{c}(\bar{c}\bar{d} - 2\bar{a}\bar{b}) + \bar{a}(\bar{a}\bar{d}+\bar{b}\bar{c})/\sqrt{2})(1+\chi_r) + \frac{\bar{d}}{2\sqrt{2}}(1-\chi_r)\},\\
\gamma_8^{(8)} &= \gamma\{(4(\bar{a}\bar{b} - \bar{c}\bar{d})^2 + 2(\bar{a}\bar{d}+\bar{b}\bar{c})^2 + \bar{a}^2/2 + \bar{c}^2/2)(1+\chi_r)\\
&+ (\bar{d}^2+\bar{b}^2)(1-\chi_r)/2\},
\end{aligned}$$

$$\gamma_5^{(9)} = \gamma_4^{(8)},\ \ \gamma_9^{(9)} = \gamma_8^{(8)},$$

$$\gamma_{10}^{(10)} = \gamma\{(4(\bar{c}\bar{d})^2 + (\bar{a}\bar{d}+\bar{b}\bar{c})^2 + \bar{a}^2/2)(1+\chi_r) + (1/2+\bar{d}^2)(1-\chi_r)/2\},$$

$$\begin{aligned}
\gamma_0^{(11)} &= 2\gamma\{(3\sqrt{2}\bar{d}\bar{c}^2 + \bar{a}(\bar{a}\bar{d}+\bar{b}\bar{c})/\sqrt{2})(1+\chi_r) + \frac{\bar{d}}{2\sqrt{2}}(1-\chi_r)\},\\
\gamma_1^{(11)} &= 2\sqrt{2}\gamma\bar{d}\bar{c}^2(1+\chi_r),\ \ \gamma_2^{(11)} = 2\gamma\{(3\sqrt{2}\bar{d}\bar{c}^2 + \bar{a}(\bar{a}\bar{d}+\bar{b}\bar{c})/\sqrt{2})(1+\chi_r)\\
&- \frac{\bar{d}}{2\sqrt{2}}(1-\chi_r)\},\\
\gamma_3^{(11)} &= 2\gamma\{(3\sqrt{2}\bar{d}\bar{c}^2 - \bar{a}(\bar{a}\bar{d}+\bar{b}\bar{c})/\sqrt{2})(1+\chi_r) + \frac{\bar{d}}{2\sqrt{2}}(1-\chi_r)\},\\
\gamma_{11}^{(11)} &= \gamma\{(4(\bar{c}\bar{d})^2 + (\bar{a}\bar{d}+\bar{b}\bar{c})^2 + \bar{a}^2/2 + 2\bar{c}^2)(1+\chi_r) + (1/2+\bar{d}^2)(1-\chi_r)/2\},
\end{aligned}$$

$$\gamma_6^{(12)} = \gamma_4^{(8)},\ \ \gamma_{12}^{(12)} = \gamma_8^{(8)},$$

$$\gamma_7^{(13)} = \gamma_4^{(8)},\ \ \gamma_{13}^{(13)} = \gamma_8^{(8)}.$$

REFERENCES

1. R. Horodecki, P. Horodecki, M. Horodecki, K. Horodecki, Rev. Mod. Phys. **81**, 865 (2009).
2. H. Ollivier, W. H. Zurek, Phys. Rev. Lett. **88**, 017901 (2001).
3. L. Henderson, V. Vedral, J. Phys. A **34**, 6899 (2001).
4. M. Piani, P. Horodecki, R. Horodecki, Phys. Rev. Lett. **100**, 090502 (2008).
5. P. Perinotti, Phys. Rev. Lett. **108**, 120502 (2012).
6. A. Ferraro, L. Aolita, D. Cavalcanti, F. M. Cucchietti, A. Acin, Phys. Rev. A **81**, 052318 (2010).
7. K. Modi, A. Brodutch, H. Cable, K. Paterek, V. Vedral, Rev. Mod. Phys. **84** 1655 (2012).
8. M. L. Hu, X. Hu, J. Wang, Y. Peng, Y. R. Zhang, H. Fan, Phys. Rep. **762-764**, 1 (2018).
9. A. Bera, T. Das, D. Sadhukhan, S. S. Roy, A. Sen (De), U. Sen, Rep. Prog. Phys. **81**, 024001 (2018).
10. B. Dakic, V. Vedral, C. Brukner, Phys. Rev. Lett. **105**, 190502 (2010).
11. W. H. Zurek, Phys. Rev. A **67**, 012320 (2003).
12. J. Oppenheim, M. Horodecki, P. Horodecki, R. Horodecki, Phys. Rev. Lett. **89**, 180402 (2002).
13. A. Datta, A. Shaji, C. M. Caves, Phys. Rev. Lett **100**, 050502 (2008).
14. B. Eastin, arXiv:1006.4402 (2010).
15. M. Piani, S. Gharibian, G. Adesso, J. Calsamiglia, P. Horodecki, A. Winter, Phys. Rev. Lett. **106**, 220403. (2011).
16. D. Cavalcanti, L. Aolita, S. Boixo, K. Modi, M.Piani, A. Winter, Phys. Rev. A **83**, 032324 (2011).
17. V. Madhok, A. Datta, Phys. Rev. A **83**, 032323 (2011).
18. A. Streltsov, H. Kampermann, D. Bruss, Phys. Rev. Lett. **106**, 160401 (2011).
19. M. Gu, H. M. Chrzanowski, S. M. Assad, T. Symul, K. Modi, T. C. Ralph, V. Vedral, P. K. Lam, Nature Phys. **8**, 671 (2012).
20. I. Ghiu, R. Grimaudo, T. Mihaescu, A. Isar, A. Messina, Entropy **22**, 785 (2020).
21. M. Calamanciuc, A. Isar, Romanian J. Phys. **65**, 119 (2020).
22. A. Dobre, A. Isar, Romanian J. Phys. **65**, 120 (2020).
23. S. Luo, S. Fu, Phys. Rev. A **82**, 034302 (2010).
24. B. Dakic, Y. O. Lipp, X. Ma, M. Ringbauer, S. Kropatschek, S. Barz, T. Paterek, V. Vedral, A. Zeilinger, C. Brukner, P. Walther, Nature Phys. **8**, 666 (2012).
25. T. Tufarelli, D. Girolami, R. Vasile, S. Bose, G. Adesso, Phys. Rev. A **86**, 052326 (2012).
26. M. Piani, Phys. Rev. A **86**, 034101 (2012).
27. X. Hu, H. Fan, D. L. Zhou, W. M. Liu, arXiv:1203.6149 (2012).
28. M. Ozawa, Phys. Lett. A **268**, 158 (2000).
29. G. Adesso, D. Girolami, Int. J. Quant. Inf. **9**, 1773 (2011).
30. G. Passante, O. Moussa, R. Laflamme, Phys. Rev. A **85**, 032325 (2012).
31. E. G. Brown, K. Cormier, E. Martin-Martinez, R. B. Mann, Phys. Rev. A **86**, 032108 (2012).
32. T. Tufarelli, T. MacLean, D. Girolami, R. Vasile, G. Adesso, J Phys. A **46**, 275308 (2013).
33. L. Jakobczyk, Phys. Lett. A **378**, 3248 (2014).
34. S. Tang, J. Yuan, L. Kuang, X. Wang, Quantum Inf. Process. **14**, 2883 (2015).
35. K. Berrada, F. Fanchini, S. Abdel-Khalek, Phys. Rev. A **85**, 052315 (2012).
36. T. Wu, J. Shi, L. Yu, J. He, L. Ye, Scientific Reports **7**, 8625 (2017).
37. M. Piani, G. Adesso, Phys. Rev. A **85**, 040301(R) (2012).
38. S. Vinjanampathy, A. R. P. Rau, J. Phys. A: Math. Theor. **45**, 095303 (2012).
39. S. Gharibian, Phys. Rev. A **86**, 042106 (2012).
40. D. Girolami, G. Adesso, Phys. Rev. Lett. **108**, 150403 (2012).

41. Z. Ficek Z and S. Swain, *Quantum Interference and Coherence: Theory and Experiments*, Springer, Berlin (2005).
42. G. S. Agarwal, *Quantum Optics*, Cambridge University Press (2014).
43. E. Cecoi, V. Ciornea, A. Isar, M. A. Macovei, J. Phys. B: At. Mol. Phys. **53**, 065501 (2020).